INDIAN JOURNAL OF SCIENCE AND TECHNOLOGY

RESEARCH ARTICLE

OPEN ACCESS
Received: 27-07-2024
Accepted: 23-12-2024
Published: 21-02-2025

Citation: Shiralashetti SC, Sangolli AM, Badiger PR (2025) Daubechies Wavelet Multigrid Method for Accurate Solution of Typical Differential Equations Arising in Hydrodynamic Lubrication Theory. Indian Journal of Science and Technology 18(6): 430-442. https://doi.org/10.17485/IJST/v18i6.2416

* **Corresponding author**.
shiralashettisc@gmail.com

Funding: None

Competing Interests: None

Published By Indian Society for Education and Environment (iSee)

ISSN
Print: 0974-6846
Electronic: 0974-5645

Daubechies Wavelet Multigrid Method for Accurate Solution of Typical Differential Equations Arising in Hydrodynamic Lubrication Theory

S C Shiralashetti[1]*, A M Sangolli[1], P R Badiger[2]

1 Department of Mathematics, Karnatak University, Dharwad, 580003, Karnataka, India
2 Department of Mathematics, Global Academy of Technology, Bengaluru, 560098, Karnataka, India

Abstract

Objectives: The present investigation is devoted to analyzing the behavior of pressure and load carrying capacity of the hydrodynamic lubrication problem. The corresponding Reynolds equation of the considered hydrodynamic lubrication problem is acquired by the application of the Stokes equations of motion to the microcontinuum theory. This modification takes into consideration the couple of stress effects that arise from the combination of various additives with the lubricant. **Method**: The Daubechies wavelet multigrid method is used to find the solution of the non-dimensional Reynolds equation. **Findings**: Initially to validate the efficiency and accuracy of the proposed strategy, the test problem is considered. The findings of the test problems are presented in tables and captured in terms of the figures to ensure that the proposed method is more accurate and consumes less computational time as compared with the Finite difference method, Multigrid Method. Later, the effect of non-dimensional pressure and load carrying capacity for the considered geometry is calculated for varied parameters. **Novelty**: Most of the lubrication problems that are available in the literature are solved by the Finite difference method and this Finite difference method has errors (truncation and roundup) and also consumes a lot of time to find the solution. In order to overcome this, the multigrid method was introduced. Again to obtain more accuracy in the solution we used the Daubechies wavelet multigrid method. When a couple stress parameters changes from 0.0 to 0.2 pressure distribution increases to 111.03%.

Keywords: Lubrication; Daubechies Wavelet Multigrid Method; Finite Journal Bearing; Couple Stresses; Reynolds Equation

1 Introduction

In the manufacture of compressors, turbines, pumps, and other machinery, journal bearings are frequently employed. If we are to prolong the life and usefulness of such equipment, the optimal operation of these moving elements is crucial. Previously, journal bearing research concentrated on the operation of bearings lubricated with Newtonian viscous fluid. Current research has revealed that adding additives to the base oil will produce a mixture with non-Newtonian behavior it will enhance the working efficiency of lubricated contacts [1,2]. Among them, the Stokes theory is regarded as the most straightforward generalization of the conventional theory of fluids because it takes polar factors like the existence of couple stresses and body couples into account. The couple stress (CS) model has been used in the theoretical investigation of lubrication issues due to its relative mathematical simplicity [3]. The coupled stress fluid model, based on Stokes microcontinuum theory, has been effectively used to explore the Rayleigh step slider bearings [4], three-lobe journal bearings [5], finite journal bearings [6], cylindrical journal bearings [7]. Dang et al. demonstrated that non-Newtonian lubricants enhance the performance of journal bearings in comparison to Newtonian lubricants [1] The authors conducted a study on squeeze film lubrication involving a rigid sphere and a flat porous plate. They discovered that the non-dimensional pressure, squeeze film time, and load carrying capacity increase as the value of CS and the viscosity parameter increase [8].

Partial differential equations (PDEs) are significant in modelling a variety of disciplines, particularly in chemistry, engineering, physics, and economics. However, determining the analytical solution to PDEs is challenging so efficient numerical methods are used. In the preceding decades, numerous methodologies have been devised, including finite difference method (FDM) [9], finite element method (FEM) [10] and spectral method (SM) [11]. These methods will convert the PDE to the system of Eqns. Wavelet analysis is a novel branch of mathematics that is widely used in image processing, numerical analysis, signal analysis, and other fields. The wavelet methods have been demonstrated to be a highly effective and efficient instrument for resolving mathematical calculus problems. These wavelets are characterized by their localization in both location and scale. In the development of precise and fast strategies for solving numerically integral and differential equations, particularly those with solutions that are highly localized in position and scale, wavelet methods have been employed. Wavelets were developed through the examination of sampling theory, wave propagation, and time-frequency signal analysis. Wavelets and wavelet transforms were discovered primarily because the Fourier transform analysis lacks the local information of signals. Spectral bases exhibit infinite differentiability but possess global support, while basis functions that are utilized in FDM or FEM have poor continuity properties but less compact support. As a result, spectral approaches perform well for spectral localization but poorly for spatial localization. Conversely, while FDM and FEM provide good spatial localization, they have problems with spectral resolution. Wavelet bases present an appealing solution by amalgamating the advantages of both spectral and finite difference (or finite element) bases. These methods will convert the PDE to the system of Eqns.

A widely used numerical method for solving large sparse linear systems of algebraic Eqns is the multigrid method (MGM). It can be used as a preconditioning strategy for other appropriate iterative methods or as an iterative solver in real-world situations. This approach explores the use of certain levels to eliminate the high-frequency or oscillatory components of the error, which are challenging to eliminate with conventional iterative methods such as Jacobi or Gauss-Seidel [12]. The utilization of wavelet bases in numerical techniques is anticipated to yield high-resolution results in both the spectral and spatial domains. Thus wavelets are used to solve PDEs [13–15]. Shiralashetti et al. employed the wavelet-Galerkin approach for the numerical solution of the Helmholtz problem using Daubechies wavelets [16]. The authors [17] solved the elastohydrodynamic lubrication problem with the help of Daubechies wavelets. The wavelet lifting approach is used to solve the numerical problem of micropolar lubrication in porous journal bearings [18]. Previously these kinds of problems were solved using the FDM so in this article we developed the Daubechies wavelet multigrid method (DWMGM) and analyzed the pressure distribution and load carrying capacity of the lubrication problem. This article is organized as follows. Mathematical preliminaries of Daubechies wavelets and Lubrication problem in Section 2. Section 3 is devoted to the DWMGM of the solution. In Section 4 the DWMGM of implementation. Section 5 provides the results and discussions. Lastly, the conclusion of the paper is presented in Section 6.

2 Mathematical preliminaries of Daubechies wavelets and Lubrication problem

Preliminaries of Daubechies Wavelets :

Wavelets are mathematical functions that simultaneously consider frequencies and resolutions they help compensate for the drawbacks of the Fourier transform. Wavelets can divide data into distinct frequency components, allowing for the scale-appropriate examination of each component at a given resolution. Constructing wavelet bases that possess desirable attributes including compact support, orthogonality, symmetry, smoothness, high order of vanishing moments, and more stands as a paramount challenge within the realm of wavelet analysis. The two functions $\Psi(x)$,the wavelet, and $\Phi(x)$,the scaling function, are used to define Daubechies wavelets. The solution to the dilation Eqn constitutes the scaling function.

$$\Phi(x) = \sqrt{2}\sum_{K=0}^{L-1} h_K \Phi(2x - K) \tag{1}$$

where $\Phi(x)$ is normalized and The scaling function is utilized to define the wavelet $\Psi(x)$, as

$$\Psi(x) = \sqrt{2}\sum_{K=0}^{L-1} g_K \Phi(2x-K). \tag{2}$$

An orthonormal basis can be constructed using $\Phi(x)$ and $\Psi(x)$ by performing functions of translation and dilation.

$$\Phi_{N,K}(x) = 2^{\frac{J}{2}}\Phi\left(2^J x - K\right) \tag{3}$$

and

$$\Psi_{N,K}(x) = 2^{\frac{J}{2}}\Psi\left(2^J x - K\right) \tag{4}$$

$H = \{h_K\}_{K=0}^{L-1}$and $G = \{g_K\}_{K=0}^{L-1}$ are related by $g_K = (-1)^K h_{L-K}$for $K = 0, 1, ..., L-1$, are referred to as quadrature mirror filters, and these parameters define all wavelet characteristics [19]. The Daubechies family of wavelets, for instance, has filter coefficients when $L = 4$as follows

$$h_0 = \frac{1+\sqrt{3}}{4\sqrt{2}}, h_1 = \frac{3+\sqrt{3}}{4\sqrt{2}}, h_2 = \frac{3-\sqrt{3}}{4\sqrt{2}}, h_4 = \frac{1-\sqrt{3}}{4\sqrt{2}}, \text{and}$$

$$g_0 = \frac{1-\sqrt{3}}{4\sqrt{2}}, g_1 = \frac{3-\sqrt{3}}{4\sqrt{2}}, g_2 = \frac{3+\sqrt{3}}{4\sqrt{2}}, g_3 = \frac{1+\sqrt{3}}{4\sqrt{2}}.$$

Daubechies wavelet multigrid operators: As a preconditioner for the DWMGM, the Daubechies wavelets transform matrix is significant. The transform matrix served as the multigrid methods restriction and prolongation operators, according to Trottenberg et al. [20]. The multigrid restriction and prolongation operators of Daubechies wavelets have a general form defined by.

$$DWR^* = \begin{bmatrix} h_0 & h_1 & h_2 & h_3 & 0 & 0 & \cdots & 0 & 0 \\ g_0 & g_1 & g_2 & g_3 & 0 & 0 & \cdots & 0 & 0 \\ 0 & 0 & h_0 & h_1 & h_2 & h_3 & \cdots & 0 & 0 \\ 0 & 0 & g_0 & g_1 & g_2 & g_3 & \cdots & 0 & 0 \\ \vdots & \vdots & & \ddots & & \ddots & \cdots & 0 & 0 \\ h_2 & h_3 & 0 & 0 & 0 & \cdots & \cdots & h_0 & h_1 \\ g_2 & g_3 & 0 & 0 & 0 & \cdots & \cdots & g_0 & g_1 \end{bmatrix}_{\frac{2^J}{2}\times 2^J} \qquad DWP^* = (DWR)'.$$

Mathematical Formulation of the Lubrication Problem :

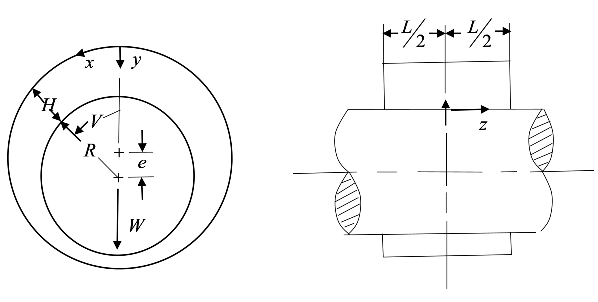

Fig 1. Physical arrangement of a pure squeeze film bearing

The geometry of an incompressible CS fluid-lubricated squeeze film bearing is depicted in Figure 1. With an assumed velocity of $\frac{dh}{dt}$, $R$is radius of nonrotating journal is getting closer to the bearing surface. Stokes microcontinuum theory is used to determine the field Eqns of an incompressible fluid with couple stresses are

$$\rho\frac{DV}{Dt} = -\nabla p + \rho B + \frac{1}{2}\nabla\times(\rho F) + (\mu - \eta\nabla^2)\nabla^2 V, \tag{5}$$

$$\nabla\cdot V = 0, \tag{6}$$

where $B, F$and $V$are vectors representing body force per unit mass, body couple per unit mass, and velocity, respectively. ρ represents density, pressure is represented by p,μ represents the classical viscosity coefficient, and η represents a new material constant responsible for the CS fluid property.

In the film region, the lubricant is characterized as an incompressible fluid with Stokes [3] CS properties. We further assume the absence of body forces and couples. Following the conventional assumptions for hydrodynamic lubrication in thin films [21], the Eqns of motion formulated by Stokes [3] assume the form

$$\frac{\partial p}{\partial x} = \mu\frac{\partial^2 v_1}{\partial y^2} - \eta\frac{\partial^4 v_1}{\partial y^4}, \tag{7}$$

$$\frac{\partial p}{\partial y} = 0, \tag{8}$$

$$\frac{\partial p}{\partial z} = \mu\frac{\partial^2 v_3}{\partial y^2} - \eta\frac{\partial^4 v_3}{\partial y^4}, \tag{9}$$

$$\frac{\partial v_1}{\partial x} + \frac{\partial v_2}{\partial y} + \frac{\partial v_3}{\partial z} = 0, \tag{10}$$

where μ, η represents lubricant viscosity, material constant respectively and (v_1, v_2, v_3) are velocity components for CS fluid. For velo Equation (11) city components, the pertinent boundary conditions (Bc's) are

at $y = 0$,

$$v_1 = 0, v_2 = 0, v_3 = 0, \frac{\partial^2 v_1}{\partial y^2} = 0 \; and \; \frac{\partial^2 v_3}{\partial y^2} = 0 \tag{11}$$

and at $y = h$,

$$v_1 = 0, v_2 = \frac{dh}{dt}, v_3 = 0, \frac{\partial^2 v_1}{\partial y^2} = 0 \; and \; \frac{\partial^2 v_3}{\partial y^2} = 0 \tag{12}$$

Equation (7) and Equation (9) are resolved by applying the Bc's from Equation (11) and Equation (12) to obtain

$$v_1 = \frac{1}{2\mu}\frac{\partial p}{\partial x}\left[y(y-H) + 2l^2\left\{1 - \frac{cosh\left[\frac{(2y-H)}{2l}\right]}{cosh\left[\frac{H}{2l}\right]}\right\}\right], \tag{13}$$

$$v_3 = \frac{1}{2\mu}\frac{\partial p}{\partial z}\left[y(y-H) + 2l^2\left\{1 - \frac{cosh\left[\frac{(2y-H)}{2l}\right]}{cosh\left[\frac{H}{2l}\right]}\right\}\right]. \tag{14}$$

Integrating Equation (10) over the film height and using Equation (13) and Equation (14) for v_1, v_3 and the use of Bc's v_2 presented in Equation (11) & Equation (12) we obtained the generalized Reynolds Eqn.

$$\frac{\partial}{\partial x}\left\{\frac{1}{12\mu}\frac{\partial p}{\partial x}\left[-H^3+12l^2\left(H-2ltanh\left(\frac{H}{2l}\right)\right)\right]\right\}+\frac{\partial}{\partial z}\left\{\frac{1}{12\mu}\frac{\partial p}{\partial z}\left[-H^3+12l^2\left(H-2ltanh\left(\frac{H}{2l}\right)\right)\right]\right\}=-\frac{dH}{dt}.$$

$$\frac{\partial}{\partial x}\left\{F(H,l)\frac{\partial p}{\partial x}\right\}+\frac{\partial}{\partial z}\left\{F(H,l)\frac{\partial p}{\partial z}\right\}=12\mu\frac{dH}{dt}, \tag{15}$$

where $F(H,l)=H^3-12l^2\left(H-2ltanh\left(\frac{H}{2l}\right)\right)$. The problem can be easily analysed by utilising the nondimensional variables and parameters in the following way.

$$\theta=\frac{x}{R},\bar{z}=\frac{z}{L},\lambda=\frac{L}{2R},\bar{l}=\frac{l}{C},\varepsilon=\frac{e}{C},\overline{H}=\frac{H}{C}=1+\varepsilon cos\theta,\overline{p}=\frac{pC^2}{\mu R^2\left(\frac{d\varepsilon}{dt}\right)}. \tag{16}$$

As a result, the modified Reynolds Eqn can be expressed in the following nondimensional form:

$$\frac{\partial}{\partial\theta}\left\{F\left(\overline{H},\bar{l}\right)\frac{\partial\overline{p}}{\partial x}\right\}+\frac{1}{4\lambda^2}\frac{\partial}{\partial\overline{z}}\left\{F\left(\overline{H},\bar{l}\right)\frac{\partial\overline{p}}{\partial\overline{z}}\right\}=12cos\theta, \tag{17}$$

where $F\left(\overline{H},\bar{l}\right)=\overline{H^3}-12\overline{l^2}\left(\overline{H}-2\bar{l}tanh\left(\frac{\overline{H}}{2\bar{l}}\right)\right)$.The bearing's ends are exposed to the surrounding pressure in the axial direction. Because negative pressure is neglected, half-film conditions are used in the circumferential direction. Consequently, the pressure Bc's for the film pressure are

$$\overline{p}=0\;at\;\overline{\theta}=\frac{\pi}{2},\frac{3\pi}{2}\;and\;\overline{p}=0\;at\;\overline{z}=\pm\frac{1}{2}. \tag{18}$$

3 Daubechies wavelet multigrid method of solution

The elliptic partial differential equations (EPDEs) are discretized using the FDM, then the resulting system of Eqns is as follows

$$QU=T. \tag{19}$$

Here Q is the $2^N\times 2^N$ coefficient matrix, T is the $2^N\times 1$ matrix, U is the $2^N\times 1$ matrix that has to be found and N is the highest level of resolution. We obtain the approximate solution S of U by solving Equation (19) iteratively. That is $U=E+S\Rightarrow S=U-E$, where E is the ($2^N\times 1$ matrix) error to be determined. There are numerous approaches to identify and reduce these errors, some of which include the multigrid method and the DWMGM. The following steps are in the DWMGM.

- We obtain the residual Eqn as $[R]_{2^N\times 1}=[T]_{2^N\times 1}-[Q]_{2^N\times 2^N}[S]_{2^N\times 1}$.
- We use the restriction operator (DWR^*) to decrease the matrices from the finer (N^{th}) level to the coarsest level ($(N-1)^{\text{th}}$), and the prolongation operator (DWP^*) is then used to generate the matrices back to the finer level from the coarsest level.

$$[R]_{2^{N-1}\times 1}=[DWR^*]_{2^{N-1}\times 2^N}[R]_{2^N\times 1},$$
$$[Q]_{2^{N-1}\times 2^{N-1}}=[DWR^*]_{2^{N-1}\times 2^N}[Q]_{2^N\times 2^N}[DWP^*]_{2^N\times 2^{N-1}}.$$

- Construct the error Eqn from the above step as $[Q]_{2^{N-1}\times 2^{N-1}}[E]_{2^{N-1}\times 1}=[R]_{2^{N-1}\times 1}$ Solve this Eqn. using an iterative method (GMRES[22]), assuming the initial guess (IG) $'0'$for $[E]_{2^{N-1}\times 1}$
- Replicate the above steps for the $(N-1)^{\text{th}}$level to $(N-2)^{\text{th}}$level.
- Repeat the process until it reaches the coarsest level, we have

$$[R]_{2\times 1} = [DWR^*]_{2\times 4}[R]_{4\times 1},$$

$$[Q]_{2\times 2} = [DWR^*]_{2\times 4}[Q]_{4\times 4}[DWP^*]_{4\times 2}.$$

As well as solving the error Eqn. $[Q]_{2\times 2}[E]_{2\times 1} = [R]_{2\times 1}$, we get $[E]_{2\times 1}$

- Now, update the solution $U_{4\times 1} = [E]_{4\times 1} + [DWP^*]_{4\times 2}[E]_{2\times 1}$. With the IG $U_{4\times 1}$ we solving $[Q]_{4\times 4}[U]_{4\times 1} = [R]_{4\times 1}$,with help of GMRES.
- Now, update the solution $U_{8\times 1} = [E]_{8\times 1} + [DWP^*]_{8\times 4}[U]_{4\times 1}$. With the IG $U_{8\times 1}$ we solving $[Q]_{8\times 8}[U]_{8\times 1} = [R]_{8\times 1}$,with help of GMRES.
- Repeat the same procedure until it reaches the finer level $U_{2^N\times 1} = [S]_{2^N\times 1} + [DWP^*]_{2^N\times 2^{N-1}}[U]_{2^{N-1}\times 1}$.
- Using the IG $U_{2^N\times 1}$, finally solve $[Q]_{2^N\times 2^N}[U]_{2^N\times 1} = [T]_{2^N\times 1}$by GMRES. The needed solution of Equation (21) using the DWMGM is obtained.

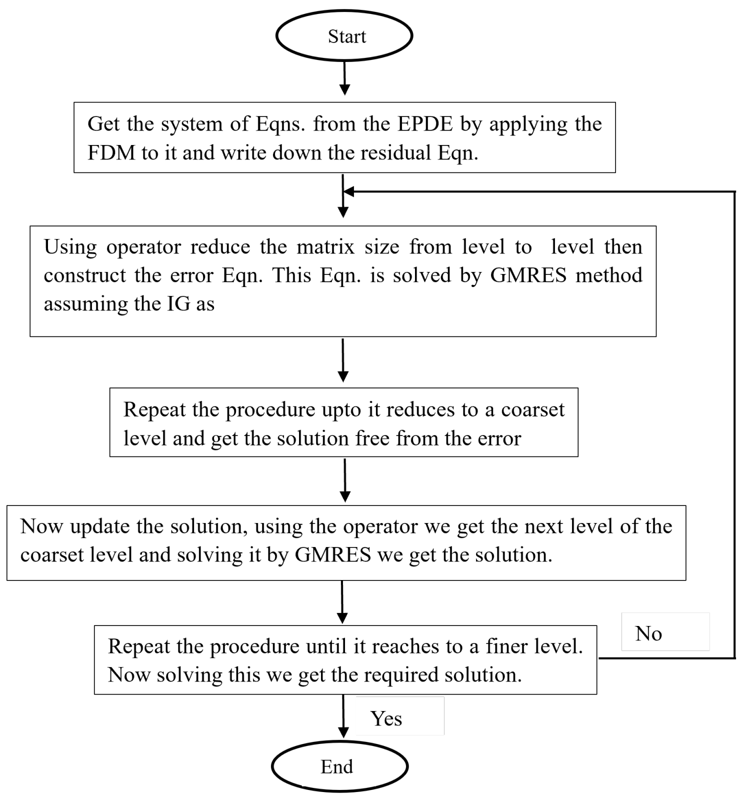

Fig 2. Flow chart of the numerical model

4 Daubechies wavelet multigrid method of implementation

In this section, we determine whether the suggested approach is effective, we first used the DWMGM for the solution of EPDEs. After that, we analysed the features of the squeeze film in finite journal bearings with the help of DWMGM.

Test Problem 4.1. Firstly we consider the EPDE [23]

$$u_{xx} + u_{yy} + 2u = 0,\ 0 \le x, y \le 1 \tag{20}$$

with Dirichlet Bc's

$$u(x,0) = sinx,\ u(x,1) = sinxcos(1), u(0,y) = 0,\ u(1,y) = sin(1)cosx \tag{21}$$

The exact solution of the test problem 4.1 is $u(x,y) = sinxcosy$. Now we apply the finite difference scheme to Equation (20) along with Bc's in Equation (21), we have

$$\frac{u_{i-1,j} - 2u_{i,j} + u_{i+1,j}}{\triangle x^2} + \frac{u_{i,j-1} - 2u_{i,j} + u_{i,j+1}}{\triangle y^2} + 2u_{i,j} = 0 \tag{22}$$

where, $i,j = 1,2,3,\ldots,N, \triangle x = x_{i+1} - x_i, \triangle y = y_{i+1} - y_i$. For our simplification consider $N = 4$, we have

$$[Q]_{16\times16}[U]_{16\times1} = [T]_{16\times1}. \tag{23}$$

Our approximation of the solution to Equation (23) using GMRES method is as follows

$[U]_{16\times1} =$ [-2.2204e-163.2719e-01 6.1837e-01 8.4147e-01 0 3.0960e-01 5.8490e-01 7.9515e-01 0 2.5753e-01 4.8648e-01 6.6130e-01 0 1.7678e-01 3.3411e-01 4.5465e-01]$'$.

- We found $[R]_{16\times1}$as

$[R]_{16\times1} =$ [2.2204e-16 2.7756e-16 -1.1102e-16 -2.2204e-16 0 2.7200e-15 -7.1054e-15 -1.1102e-16 0 5.5511e-16 -2.2204e-16 -2.2204e-16 0 -2.7756e-17 -5.5511e-17 -5.5511e-17]'.

- We have $[R]_{8\times1} = [DWR^*]_{8\times16}[R]_{16\times1}$and $[Q]_{8\times8} = [DWR^*]_{8\times16}[Q]_{16\times16}[DWP^*]_{16\times8}$.
- The error Eqn is constructed as$(Q]_{8\times8}(E]_{8\times1} = (R]_{8\times1}$, and it is solved using GMRES while taking the IG "0" into consideration. The outcomes are as follows.

$[E]_{8\times1} =$ [3.4327e-16 -7.6580e-17 -2.4484e-16 4.3716e-17 8.5915e-17 1.7916e-16 -1.2983e-17 1.1236e-17]$'$

- Replicate the above steps for the 3rd level to 2nd level.
- Repeating the process until it reaches to the coarsest level, we have $[R]_{2\times1}$ = [-4.7118e-16 -2.2841e-15]$'$, and $Q = \begin{bmatrix} 9.4747e-01 & -1.8740e+00 \\ -1.3115e+00 & -2.0982e+01 \end{bmatrix}$. Now we were able to determine the error Eqn as, $\begin{bmatrix} 9.4747e-01 & -1.8740e+00 \\ -1.3115e+00 & -2.0982e+01 \end{bmatrix} [E]_{2\times1} = \begin{bmatrix} -4.7118e-16 \\ -2.2841e-15 \end{bmatrix}$solving this error Eqn by GMRES, we get $[E]_{2\times1}$ = [-2.5097e-16 1.2455e-16]$'$.
- Now, update the solution $U_{4\times1}$ = [-2.0602e-16 -1.1758e-15 4.1584e-15 2.0730e-15]$'$.With the IG $U_{4\times1}$ = [-2.0602e-16 -1.1758e-15 4.1584e-15 2.0730e-15]$'$ we solving $[Q]_{4\times4}[U]_{4\times1} = [R]_{4\times1}$,with help of GMRES.
- Now, update the solution

$U_{8\times1}$ = [3.4327e-16 -7.6580e-17 -2.4484e-16 4.3716e-17 8.5915e-17 1.7916e-16 -1.2983e-17 1.1236e-17]$'$.
With the IG
$U_{8\times1}$ = [3.4327e-16 -7.6580e-17 -2.4484e-16 4.3716e-17 8.5915e-17 1.7916e-16 -1.2983e-17 1.1236e-17]$'$.
we solving $[Q]_{8\times8}[U]_{8\times1} = [R]_{8\times1}$,with help of GMRES.

- Repeating the same procedure until it reaches the finer level we get

$U_{16\times1}$ = [-4.6348e-17 3.2719e-01 6.1837e-01 8.4147e-01 8.1937e-30 3.0960e-01 5.8490e-01 7.9515e-01 6.4895e-18 2.5753e-01 4.8648e-01 6.6130e-01 0 1.7678e-01 3.3411e-01 4.5465e-01]$'$.

- Using the IG $U_{16\times1}$, finally solve $(Q]_{16\times16}(U]_{16\times1} = (T]_{16\times1}$ by GMRES. The needed solution of Equation (20) using the DWMGM is presented in Figure 3 and Table 1 shows the maximum error and CPU time required to compute the solutions.

Test Problem 4.2 . Secondly we consider the EPDE [24]

$$\frac{\partial^2 z}{\partial x^2} + \frac{\partial^2 z}{\partial y^2} = 10\,(x-1)\,cos(5y) - 25\,(x-1)\,(y-1)\,sin(5y), 0 \le x, y \le 1. \tag{24}$$

with Dirichlet Bc's

$$z\,(x,0) = 0, z\,(x,1) = 0, z\,(0,y) = (1-y)\,sin\,(5y)\,, z\,(1,y) = 0. \tag{25}$$

The exact solution of the test problem 4.2 is $z\,(x,y) = (1-x)\,(1-y)\,sin(5y)$.Equation (24) reduces to the linear system by applying the finite difference approximations of the derivatives. Using the DWMGM described in section 3, the resultant numerical solution to test problem 4.2 is shown in Figure 4 and in Table 2, the maximum error and CPU time required to compute the solutions are shown.

5 Results and discussions

Table 1. Compares the maximum error and CPU time (in seconds) of FDM, MGM, and D WMGM for test problem 4.1

Size of the Matrices	Numerical Method	$E_{\max.}$	Time		
			Setup	Running	Total
16×16	FDM MGM DWMGM	5.6469e-04 5.6469e-04 5.6469e-04	2.5070e+00 1.0332e-01 2.3860e-02	4.2553e-02 5.6556e-03 1.8134e-03	2.5495e+00 1.0897e-01 2.5673e-02
64×64	FDM MGM DWMGM	1.1747e-04 1.1747e-04 1.1747e-04	2.7823e+00 1.5348e-01 4.8092e-02	6.2863e-02 6.4056e-03 2.4858e-03	2.8451e+00 1.5989e-01 5.0578e-02
256×256	FDM MGM DWMGM	2.6061e-05 2.6061e-05 2.6061e-05	4.5244e+00 2.6403e-01 6.8598e-02	5.0378e-02 5.1116e-03 1.6016e-03	4.5748e+00 2.6914e-01 7.0200e-02
1024×1024	FDM MGM DWMGM	6.1113e-06 6.1113e-06 6.1113e-06	2.9096e+00 4.7330e-01 2.4198e-01	2.3927e-01 1.0233e-02 7.0852e-03	3.1489e+00 4.8353e-01 2.4906e-01

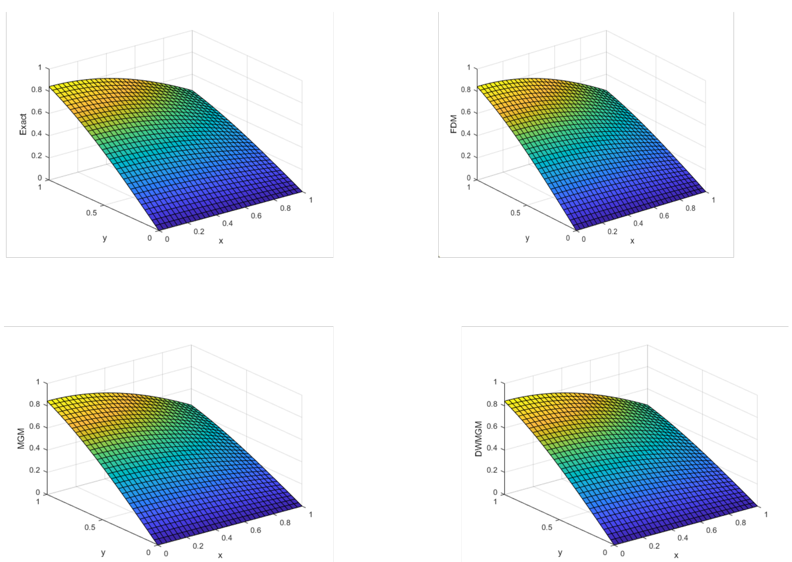

Fig 3. Shows the solution of exact, FDM, MGM, and DWMGM to Test Problem 4.1

Table 2 shows that when the order of the matrix grows, the maximum error reduces, and the CPU time of DWMGM is lower than that of FDM and MGM.

Table 2. Compares the maximum error and CPU time (in seconds) of FDM, MGM, and DWMGM for test problem 4.2

Size of the Matrices	Numerical Method	$E_{\mathbf{max}.}$	Time		
			Setup	Running	Total
16×16	FDM MGM DWMGM	8.1855e-02 8.1855e-02 8.1855e-02	7.0728e+00 1.5237e-01 3.4676e-02	4.9843e-01 4.6801e-03 9.5822e-03	7.5712e+00 1.5705e-01 4.4258e-02
64×64	FDM MGM DWMGM	1.4283e-02 1.4283e-02 1.4283e-02	2.6039e+00 1.4691e-01 4.2212e-02	6.7784e-02 5.9385e-03 4.8316e-03	2.6717e+00 1.5285e-01 4.7043e-02
256×256	FDM MGM DWMGM	3.0963e-03 3.0963e-03 3.0963e-03	3.7386e+00 3.0885e-01 8.2227e-02	5.6260e-02 5.9144e-03 2.1758e-03	3.7948e+00 3.1476e-01 8.4403e-02
1024×1024	FDM MGM DWMGM	7.2588e-04 7.2588e-04 7.2588e-04	4.1792e+00 4.1408e-01 2.2376e-01	2.3690e-01 4.5105e-03 6.8268e-03	4.4161e+00 4.1859e-01 2.3059e-01

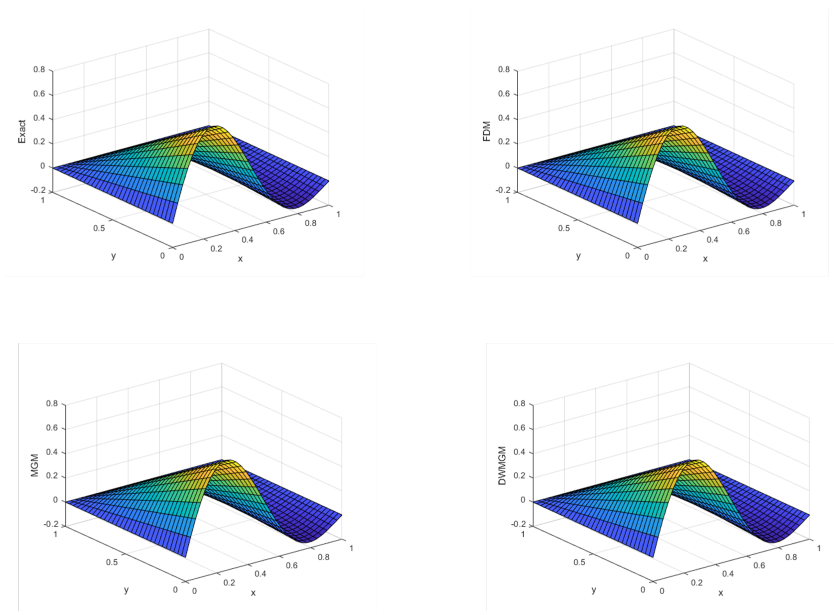

Fig 4. Shows the solution of exact, FDM, MGM, and DWMGM to Test Problem 4.2

Pressure variation:

Non-dimensional Reynolds Equation (17) is solved by DWMGM with the help of Bc's Equation (18) . The fluctuation of non-dimensional squeeze film pressure $\left(\overline{P}\right)$ with the circumferential coordinate θ for different values of CS parameter $\left(\bar{l}\right)$ and eccentricity ratio (ε) is represented in the Figure 5. It has been seen that $\overline{P}$ increases as $\bar{l}$ values increase. Moreover, the CS effects increase with the increase in values of ε.Figure 6 shows how the non-dimensional squeeze film pressure varies with the circumferential coordinate for various values of the length-to diameter ratio (λ) and CS parameter. The bearing with the length-to-diameter ratio $\lambda = 1.5$ exhibits more pronounced effects of couple stresses on the film pressure. The couple stress parameter in lubrication theory accounts for microstructural behaviour in non-Newtonian fluids, resulting in improved load support, increased film thickness, reduced friction, and enhanced stability across various lubrication regimes. This characteristic is particularly important for sophisticated lubricants made for harsh environments or small-scale uses.

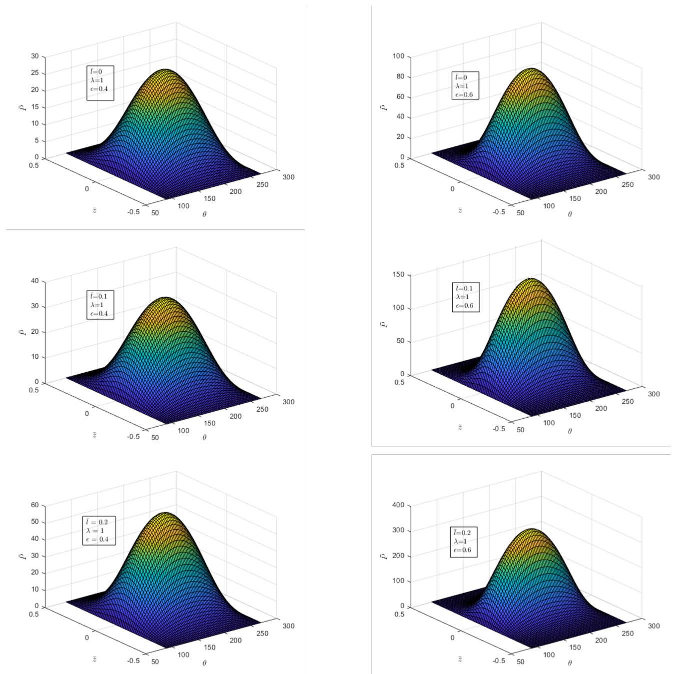

Fig 5. The non-dimensional film pressure fluctuation with circumferential coordinates for various values of $\bar{l}$ and $\varepsilon$with $\lambda = 1$

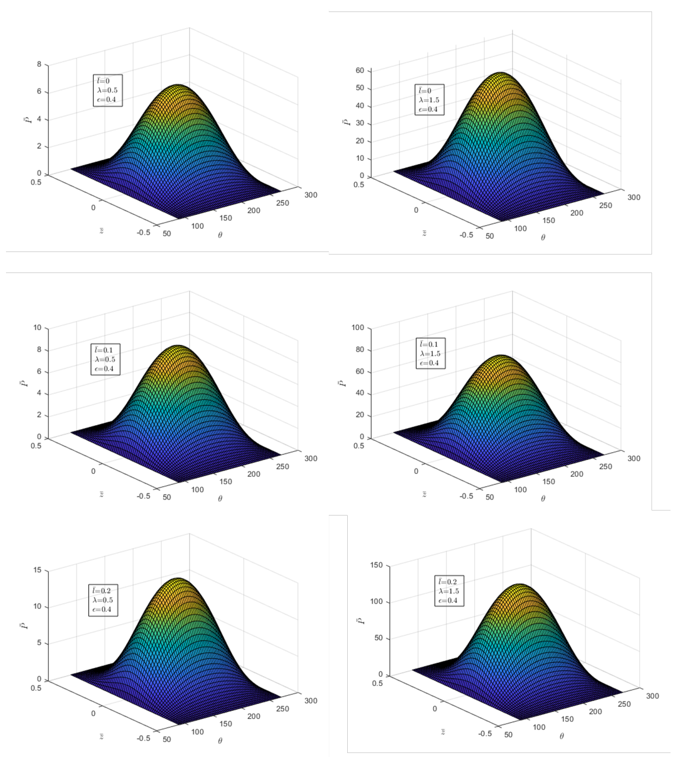

Fig 6. The variation of non-dimensional film pressure with circumferential co-ordinate for different values of λ with $\varepsilon = 0.4$

Load-carrying capacity:

Squeeze bearing load carrying capacity is expressed as the integral of the film pressure acting on the journal.

$$W = -2R\int_{z=0}^{z=\frac{L}{2}} \int_{\theta=\frac{\pi}{2}}^{\theta=\frac{3\pi}{2}} P cos\theta d\theta dz. \tag{26}$$

We introduce the dimensionless quantity

$$\overline{W} = \frac{WC^2}{\mu LR^3 \frac{d\varepsilon}{dt}}. \tag{27}$$

Dimensionless load-carrying capacity is given by

$$\overline{W} = -\Delta\theta\Delta\overline{z}\sum_{i=0}^{m}\sum_{j=0}^{n}\overline{P}_{i,j}cos\theta_i. \tag{28}$$

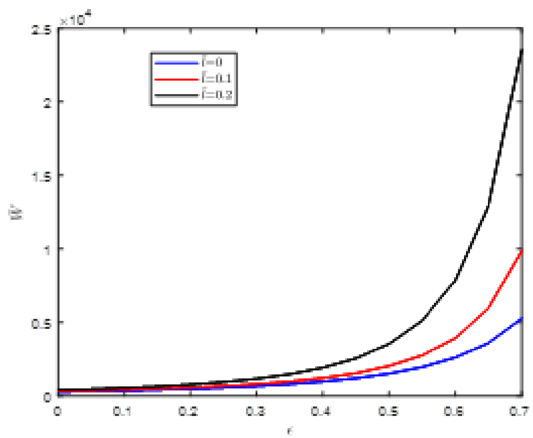

Fig 7. Distribution of dimensionless $\overline{W}$ with ε for various values of $\overline{l}$ under $\lambda = 1$

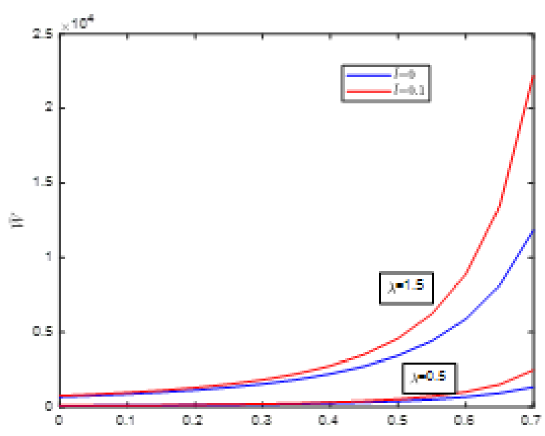

Fig 8. Effect of λ on dimensionless $\overline{W}$ versus ε

Figure 7 shows the fluctuation of the dimensionless load carrying capacity $\overline{W}$ with the eccentricity ratio $\varepsilon$for various values of the CS parameter $\overline{l}$ with$\lambda = 1$. As the CS parameter is increased, it can be seen that the load carrying capacity increases compared to the Newtonian situation. Additionally, it is observed that as values of ε increase the load carrying capacity rises. Figure 8 displays the effect of λ on $\overline{W}$ versus ε. It is observed that as λ value increases the load carrying capacity is also increased in both Newtonian and non-Newtonian cases.

6 Conclusion

This study delves into the impact of couple stresses on the performance of finite journal bearings operating under pure squeeze film conditions, with a foundation rooted in the principles of the Stokes microcontinuum theory. The modified Reynolds Eqn is derived from the microcontinuum theory by applying the Stokes Eqns of motion to account for the CS effects caused by the lubricant combined with various additives. The proposed method is more accurate and consumes less computational time as compared with the FDM, MGM. We applied the proposed Daubechies wavelet method to solve this Reynolds Eqn. Dimensionless pressure increases with an increase in the CS parameter and eccentricity ratio. The load carrying capacity of the bearing is also increased as a length-to-diameter ratio and CS parameter increases. Additionally, the proposed technique can be expanded to address divergent lubrication-related problems.

Acknowledgements

The authors thank University Grants Commission (UGC), New Delhi, for supporting this work partially through UGC-SAP DRS-III for 2016-2021: F.510/3/DRS-III/2016 (SAP-I). Also thankful to the Council of Scientific and Industrial Research, New Delhi for the Junior Research Fellowship: File No. 09/101(0060)/2020-EMR-I.

References

1) Dang RK, Goyal D, Chauhan A, Dhami SS. Effect of non-Newtonian lubricants on static and dynamic characteristics of journal bearings. *Materials Today: Proceedings*. 2020;28:1345–1349. Available from: https://doi.org/10.1016/j.matpr.2020.04.727.
2) Patil SM, Vinay CV, Dinesh PA. Numerical approach to interpret the attributes of porous journal bearings using couple-stress fluid. *Industrial Lubrication and Tribology*. 2021;73(2):253–259. Available from: https://doi.org/10.1108/ILT-02-2020-0051.
3) Stokes VK. Couple stresses in fluids. In: and others, editor. Theories of Fluids with Microstructure;vol. 9. Berlin, Heidelberg. Springer. 1984;p. 34–80.
4) Naduvinamani NB, Ganachari R. Double Layered porous Rayleigh step slider bearings lubricated with couple stress fluids. *Indian Journal of Science and Technology*. 2022;15(28):1389–1398. Available from: https://indjst.org/articles/double-layered-porous-rayleigh-step-slider-bearings-lubricated-with-couplestress-fluids.
5) Chetti B, Crosby WA. Preload effects on the static characteristics of three-lobe journal bearings lubricated with a couple stress fluid. *Industrial Lubrication and Tribology*. 2019;71(10):1136–1143. Available from: https://doi.org/10.1108/ILT-12-2018-0435.
6) Dass T, Gunakala SR, Comissiong DM. The combined effect of couple stresses, variable viscosity and velocity-slip on the lubrication of finite journal bearings. *Ain Shams Engineering Journal*. 2020;11(2):501–518. Available from: https://www.sciencedirect.com/science/article/pii/S2090447920300046.
7) Lambha SK, Kumar V, Verma R. Elastohydrodynamic analysis of couple stress lubricated cylindrical journal bearing. *In Journal of Physics: Conference Series*. 2019;1240(1). Available from: https://iopscience.iop.org/article/10.1088/1742-6596/1240/1/012165.
8) Hanumagowda BN, Sreekala CK, Noorjahan N, Makinde OD. Squeeze film lubrication on a rigid sphere and a flat porous plate with Piezo-viscosity and couple stress fluid. *Defect and Diffusion Forum*. 2020;401:140–147. Available from: https://doi.org/10.4028/www.scientific.net/DDF.401.140.
9) Ghosh S, Niranjanamurthy M, Deyasi K, Mallik BB, Das S. Mathematics and Computer Science;vol. 2. and others, editor;John Wiley & Sons. 2023. Available from: https://www.wiley.com/en-ae/Mathematics+and+Computer+Science%2C+Volume+2-p-9781119896326.
10) Gokul KC, Dulal RP. Adaptive finite element method for solving Poisson partial differential equation. *Journal of Nepal Mathematical Society*. 2021;4(1):1–18. Available from: https://www.researchgate.net/publication/351593491_Adaptive_Finite_Element_Method_for_Solving_Poisson_Partial_Differential_Equation.
11) Arendt W, Urban K. Partial Differential Equations: An Introduction to Analytical and Numerical Methods;vol. 294. 1st ed. and others, editor;Springer Nature. 2023. Available from: https://doi.org/10.1007/978-3-031-13379-4.
12) Shojaei I, Rahami H. A new numerical solution for system of linear equations. *Journal of Algorithms and Computation*. 2021;53(1):23–39. Available from: https://journals.ut.ac.ir/article_81267_23db04a9319ce7c9f6bbf2eb577623b4.pdf.
13) Li Y, Xu L, Ying S. DWNN: deep wavelet neural network for solving partial differential equations. *Mathematics*. 2022;10(12). Available from: https://www.mdpi.com/2227-7390/10/12/1976.
14) Shiralashetti SC, Hanaji SI. Taylor wavelet collocation method for Benjamin-Bona-Mahony partial differential equations. *Results in Applied Mathematics*. 2021;9. Available from: https://www.sciencedirect.com/science/article/pii/S2590037420300492.
15) Shiralashetti SC, Angadi LM, Deshi AB. Numerical solution of some class of nonlinear partial differential equations using wavelet-based full approximation scheme. *International Journal of Computational*. 2020;17(6):1–23. Available from: https://www.researchgate.net/publication/331039697_Numerical_Solution_of_Some_Class_of_Nonlinear_Partial_Differential_Equations_Using_Wavelet-Based_Full_Approximation_Scheme.
16) Shiralashetti SC, Kantli MH, Deshi AB. New wavelet-Galerkin method for the numerical solution of Helmholtz equation. *Palestine Journal of Mathematics*. 2021;10(2):732–739. Available from: https://pjm.ppu.edu/sites/default/files/papers/PJM_June_2021_732to739.pdf.
17) Shiralashetti SC, Hanaji SI, Naregal SS. Daubechies wavelet based numerical method for the solution of grease elastohydrodynamic lubrication problem. *AIP Conference Proceedings*. 2020;2246(1). Available from: https://pubs.aip.org/aip/acp/article-abstract/2246/1/020029/727421/Daubechies-wavelet-based-numerical-method-for-the?redirectedFrom=PDF.
18) Shiralashetti SC, Badiger PR. Wavelet lifting method for the numerical solution of micropolar lubrication problem of porous journal bearing. *International Journal of Ambient Energy*. 2023;44(1):2446–2458. Available from: https://www.tandfonline.com/doi/abs/10.1080/01430750.2023.2247397.

19) Daubechies I. Orthonormal bases of compactly supported wavelets. *Communications on Pure and Applied Mathematics*. 1988;41(7):909–996. Available from: https://doi.org/10.1002/cpa.3160410705.
20) Trottenberg U, Oosterlee CW, Schuller A. Multigrid. 1st ed. London. Academic Press. 2000. Available from: https://shop.elsevier.com/books/multigrid/trottenberg/978-0-08-047956-9.
21) Pinkus O, Sternlicht B, Saibel E, Journal of Applied Mechanics. Theory of Hydrodynamic Lubrication;vol. 29. and others, editor. 1962. Available from: https://www.semanticscholar.org/paper/Theory-of-Hydrodynamic-Lubrication-Pinkus-Sternlicht/c8f4ec27583e5c9f4e17821108a01e934a39d100.
22) Jude D, Sitaraman J, Lakshminarayan V, Baeder J. An overset generalised minimal residual method for the multi-solver paradigm. *International Journal of Computational Fluid Dynamics*. 2020;34(1):61–74. Available from: https://dx.doi.org/10.1080/10618562.2019.1710137.
23) Liu M, Hou M, Wang J, Cheng Y. Solving two-dimensional linear partial differential equations based on Chebyshev neural network with extreme learning machine algorithm. *Engineering Computations*. 2021;38(2):874–894. Available from: https://www.emerald.com/insight/content/doi/10.1108/ec-08-2019-0387/full/html.
24) Elsherbeny AM, El-hassani RMI, El-badry H, Abdallah MI. Solving 2D-Poisson equation using modified cubic B-spline differential quadrature method. *Ain Shams Engineering Journal*. 2018;9(4):2879–2885. Available from: https://dx.doi.org/10.1016/j.asej.2017.12.001.